IEEE Access
Multidisciplinary | Rapid Review | Open Access Journal

Received July 28, 2019, accepted August 20, 2019, date of publication August 27, 2019, date of current version September 18, 2019.

Digital Object Identifier 10.1109/ACCESS.2019.2937833

Stratified Optimization Strategy Used for Restoration With Photovoltaic-Battery Energy Storage Systems as Black-Start Resources

JUNHUI LI[1], (Member, IEEE), HONGFEI YOU[1], JUN QI[2], MING KONG[3], SHINING ZHANG[1], AND HONGGUANG ZHANG[2]

[1]Key Laboratory of Modern Power System Simulation and Control & Renewable Energy Technology, Ministry of Education (Northeast Electric Power University), Jilin 132012, China
[2]The Operation Department of Electric Power Dispatching Center, Inner Mongolia Power (Group) Co., Ltd., Hohhot 010020, China
[3]Jinan Power Supply Bureau, State Grid Shandong Electric Power Company Ltd., Jinan 250000, China

Corresponding author: Junhui Li (lijunhui@neepu.edu.cn)

This work was supported in part by the National Natural Science Foundation of China under Grant U1766204, and in part by the Special Fund for Industrial Innovation of Jilin Province Development and Reform Commission under Grant 2017C017-2.

ABSTRACT With the rapid growth of installed capacity of photovoltaic (PV), the PV power stations equipped with energy storage (ES) have become a new type of black-start power supply. Taking the Photovoltaic-Battery Energy Storage Systems (PV-BESS) as the black-start power source can improve the black-start ability of the regional power grid and broaden the application prospect of PV power generation. In this paper, a stratified optimization strategy for black-start of PV-BESS is proposed, which combines the key issues in the process of black-start of PV-BESS. Stratified optimization strategy is divided into data analysis layer, optimization coordination layer and scheduling control layer. The data analysis layer combines the requirements of the black-start process. Firstly, the similarity matrix ranking method is used to improve the PV power prediction method. Secondly, based on probability inclination, the PV power index is designed to evaluate the feasibility of black-start by calculating the PV lower limit power and the executable probability inclination. The optimization coordination layer is based on the state space model of black-start of PV-BESS, combined with the control strategy of PV as the main part and ES as the auxiliary part, the optimization objectives of the maximum utilization rate of PV and tracking the ideal value of state of charge (SOC) of ES is formulated. The optimal model is solved by model predictive control, and the output power of PV and ES is controlled to complete the black-start process. The actual historical data in the power grid with a high proportion of PV sources are used as the basic data for simulation. The simulation of black-start based on MATLAB/Simulink verifies the rationality of the stratified optimization strategy, which provides a reference for the realization of black-start of PV-BESS.

INDEX TERMS Black-start, stratified optimization strategy, photovoltaic-battery energy storage systems, photovoltaic & energy storage coordination, photovoltaic power prediction.

NOMENCLATURE

PV	Photovoltaic
ES	Energy storage
PV-BESS	Photovoltaic-Battery Energy Storage Systems
LSSVM	Least squares support vector machine
MPC	Model predictive control
SVM	Support vector machines
N_r	The number of PV units
P_{ESS}	The charge/discharge power of ES(kW)
$P_{PV-unit}$	The predicted output power of PV unit(kW)
P_L	The auxiliary power of thermal power units(Load power of black-start) (kW)
P_{PV}	The total PV power
SOC	state of charge
P_{PV-lim}	The lower limit of PV units power(kW)

The associate editor coordinating the review of this article and approving it for publication was Eklas Hossain.

η	The executive probability inclination of black-start
N	The total number of PV units in PV power stations
NWF	Numerical weather forecast
x_{dk}	The solar radiation intensity or temperature of d-day in historical day
x_k	The solar radiation intensity or temperature of the day to be predicted
n	The sampling point of the solar radiation intensity and temperature in a day
M	The similarity matrix
m_{id}	The similarity between each factor affecting the d-day and the predicted day.
F_d	The total similarity between the d-th historical day and the day to be predicted
R	The correlation coefficient
T	The black-start period
x(k)	The state variables at k time
u(k)	The control variables at k time
r(k)	The disturbance input at k time
y(k)	The output variables at k time
$P_{PV}(k)$	The total PV power at k time(kW)
$P_{PV-unit}(k)$	The power prediction value of PV units at k time(kW)
$P_{PV-unit}(k+1)$	The predicted PV unit power at k+1 time(kW)
$P_{PV-unitN}$	The rated power of PV units(kW)
$P_{ESS}(k)$	The charge/discharge power of ES at k time(kW)
$E_{ESS}(k)$	The capacity actually collected at k time(kWh)
$E_{ESS}(k+1)$	The ES capacity at k+1 time(kWh)
E_{ESSL}	The ideal capacity of ES(kWh)
P_L (k)	The load power at k time(kW)
$P_L(k+1)$	The load power at k+1 time(kW)
ΔT_{ESS}	The conversion coefficient from kW to kWh
$N_r(k)$	The number of PV units actually collected at k time
$N_r(k+1)$	The number of PV units actually collected at k+1 time
ΔN_r	The change value of PV unit number
ΔP	The compensation power(kW)
P_{ESSN}	The rated power of ES
SOC_{max}	The upper limit of SOC of ES
SOC_{min}	The lower limit of SOC of ES
SOC (k)	The SOC of ES at k time
M	The rolling period
β	The change limit of the number of PV units

I. INTRODUCTION

In recent years, several large-area blackouts have taken place in the United States, Italy, China, India, Brazil and other places [1]–[3]. The blackout in India on 30 July 2012 directly affected the lives of more than 600 million people, which are the largest power failure affecting the population in history [4]. In March 2018, the 3.21 blackout in Brazil affected more than 53 million people, more than a quarter of the national population, and caused 9300 MW of blackout load loss. Large blackouts bring huge losses to the national economy. Black-start, the procedure to restore the power supply by self-starting black start units (BSU), is the first task after a severe blackout occurs [2], [3]. Fast and effective black-start schemes can minimize the losses brought about by large blackouts in power grids [5], [6].

Conventional black-start schemes use hydropower turbine and gas turbine with great self-starting ability as black-start sources, and relevant experiments have been carried out in [7], [8]. Reference [9] presented the black-start experiment using pumped-storage units as the power supply in the Shandong power grid, China. Reference [10] analyzed the black-start experiment using hydropower turbine and gas turbine as the power supply in India. However, the uneven distribution of water resources and the lack of water resources in some areas limit the construction of hydropower units; gas turbines require high-power diesel generator sets to provide start-up power and need to be turned on regularly for maintenance. The high investment cost is not appropriate for widespread use. Therefore, the participation of renewable energy in the black-start process can effectively utilize natural resources and select different black-start power sources according to the distribution of resources in different regions [11], [12]. Reference [13] chose micro-grid as black-start power supply and proposed an optimized restoration method for a distribution network. A control method is proposed for the power quality problem of micro-grid used as the black-start source for [14], [15]. The participation of renewable energy sources will greatly accelerate the process of black-start development.

Nowadays, the installed capacity of PV is increasing year by year [16], [17]. ES technology and PV power generation technology are developing rapidly. For areas with abundant lighting resources, more and more studies have been done on the participation of PV power generation systems in power system restoration. Reference [18] proposes an optimization method to improve the restoration efficiency of the power grid by using PV power plant as a black-start power supply. In reference [19], a black-start strategy based on hierarchical control is proposed for micro-grid with PV-BESS, which improves the black-start capability of micro-grid. Because of the fluctuation of PV power generation, it is necessary to configure ES to suppress the fluctuation of PV output power [16], [20]. Reference [21], [22] studies the control strategy of PV-BESS under island operation mode, ES provides stable voltage and frequency for PV inverters. Reference [23] presents a method to reduce the fluctuation of PV power by hybrid ES. The black-start capability of a micro-grid is enhanced by configuring ES in the micro-grid [24]. The above research shows that the PV-BESS offers the opportunity to act as a black-start power supply.

When the PV-BESS is used as black-start power supply, because of the randomness and uncertainty of PV power generation [25], [26], the PV-BESS can only be the black-start power supply in the executable period. Before the start of a black-start process, it is necessary to determine whether the PV-BESS is in the executable black-start period. The influence of uncertainty of renewable generation on the black-start process has been considered in previous studies. In reference [27], the access time and capacity of wind power are determined by the black-start value evaluation method to determine whether the output power of wind power meets the requirements of the black-start process. However, reference [27] regards wind power as an auxiliary black-start power source. After the main black-start power source has formed a small stable parallel system with the thermal power unit, the follow-up process is accelerated by connecting wind power. It is not suitable for the black-start process of the main black-start power supply of wind power. In the process of black-start of a micro-grid, reference [28] models the uncertainty of black-start of micro-grid by discretizing the probability distribution of prediction error and chooses typical scenarios of black-start of the micro-grid to establish probability function to determine the reference value of output power of micro-grid. However, in reference [28], whether renewable energy generation supports black-start process has not formed a quantitative standard, which is not appropriate for the black-start of PV-BESS. Reference [29] introduced a black-start power supply selection method for renewable energy generation systems in distribution networks. A renewable energy source which can assist the black start process is chosen by power prediction and maximum likelihood estimation. However, reference [29] divides the large power grid into several small power grids for service recovery, aiming at the maximum priority load recovery, which does not apply to the feasibility assessment of specific systems. The reference value of PV power can be obtained by PV power prediction technology [30].

Because the ES device with charge/discharge power constraint and capacity constraint, when the PV output is insufficient or fluctuates violently during the black-start process, there may be over-charging and over-discharging of ES, which leads to the failure of the black-start. Also, the auxiliary load changes frequently, so the energy coordination control in black-start becomes more complex. How to coordinate the output of PV and ES to ensure adequate load supply and keep the SOC of ES at a reasonable level directly determines the success of black-start. Reference [31] combines load tracking with maximum power point tracking control to effectively control PV output power and complete the black-start process. However, in the process of choosing the PV control strategy, the SOC of ES is not taken into account, which may lead to over-charging and over-discharging of energy storage. In reference [19], a black-start strategy based on hierarchical control is proposed for PV/ES micro-grid. Different control strategies are applied to single-phase micro-grid and three-phase micro-grid respectively to coordinate the output power of PV and ES to achieve black-start. However, the method proposed in reference [19] is to assist three-phase micro-grid with black-start through single-phase micro-grid, which is not suitable for single PV-BESS. Reference [28] proposes an optimization strategy for black-start power supply based on MPC to reduce the time spent in the black-start process by controlling the starting sequence of black-start units. However, reference [28] solves a planning problem for black-start of a micro-grid, which does not specify the coordinated control between black-start power sources and is not suitable for the coordinated control of PV and ES. In the above study, no research has been carried out on the problems in the process of the black-start of PV-BESS.

The above research on black-start of PV-BESS is to take PV power generation as part of the micro-grid and the whole micro-grid as the black-start power supply. Without considering the black-start power supply of PV-BESS, the feasibility of black-start of PV-BESS and the coordinated control of PV and ES are studied. Therefore, a stratified optimization strategy for black-start of PV-BESS is proposed in this paper. The stratified optimization strategy is divided into data analysis layer, optimization coordination layer and scheduling control layer. The data analysis layer combines with the requirements of the black-start process. Firstly, based on the similarity matrix sorting method, the training sample selection method of the PV power prediction method is improved, and the PV power prediction method suitable for a black-start process is obtained. Based on the reference value of the PV output power obtained from the prediction, the lower limit power of PV and the executable probability inclination are calculated. To evaluate the feasibility of black-start of PV-BESS. In the optimization coordination layer, the control strategy of PV as the main part and ES as the auxiliary part is formulated. Based on the mathematical model of black-start of PV-BESS, the optimal number of PV cells and the charge/discharge power of ES are obtained through MPC to solve the optimization objective. The actual historical data of the actual power grid are taken as the basic data of simulation, black-start simulation based on MATLAB is carried out to verify the effectiveness and rationality of the proposed strategy.

The remainder of this paper is organized as follows: Section II introduces the black-start process of PV-BESS and describes the structure of black-start of PV-BESS. Section III presents the stratified optimization strategy for black-start of PV-BESS. Section IV is to verify the effectiveness of the strategy by simulation. Finally, key conclusions are offered in Section V.

II. PV-BESS USED FOR BLACK-START

A. BLACK-START PROCESS OF PV-BESS

After the PV power station receives the black start instruction, Firstly, the output power of PV power station is evaluated to determine the feasibility of black-start of PV-BESS. After determining that the output power of PV power station can meet the requirements of black-start. Second, the ES assist

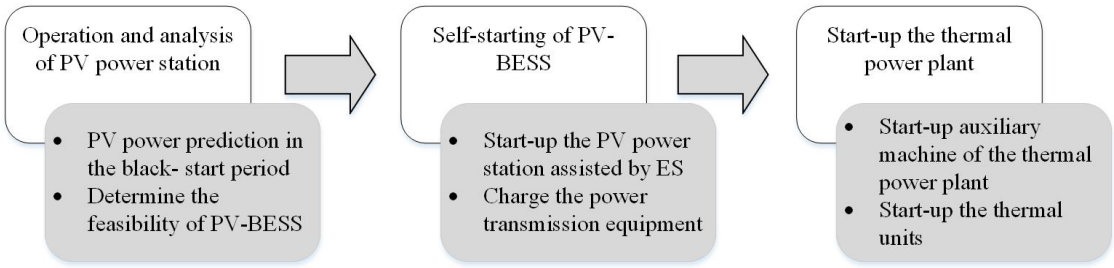

FIGURE 1. The black-start process of power grid based on PV-BESS.

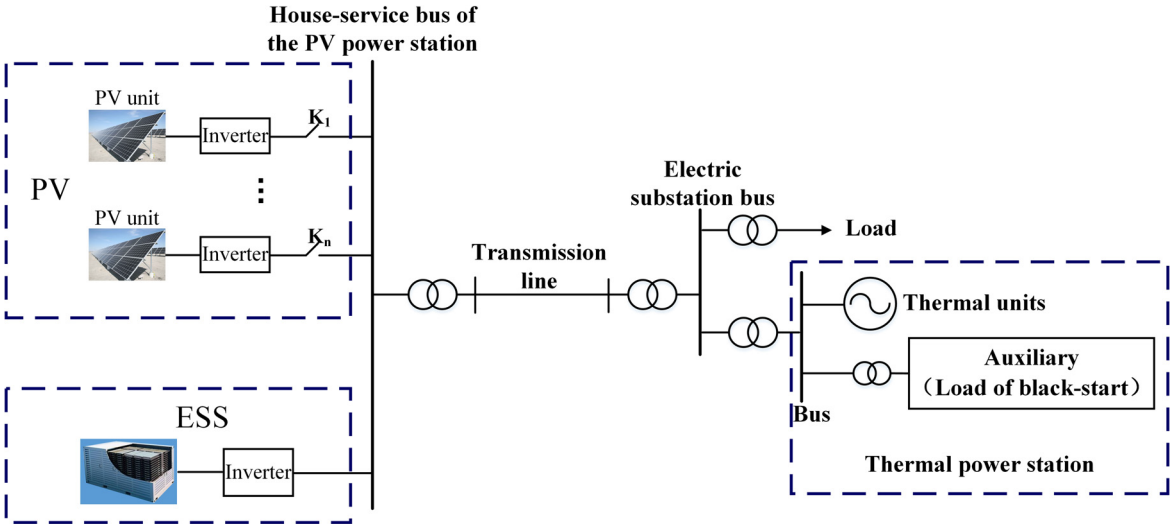

FIGURE 2. Structural of black-start system with the PV-BESS as main power supply. The PV-BESS is mainly composed of PV and ESS. The PV-BESS as black-start power to start auxiliaries of thermal power station.

the start-up of the PV power station, and the PV-BESS will be used as the black-start power source to charge the transmission line. Finally, the PV-BESS gradually starts the auxiliary engine of the thermal power plant until the output power of the whole thermal power plant resumes.

The black-start process of power grid based on PV-BESS is shown in Fig. 1.

B. STRUCTURE OF PV-BESS

The PV-BESS is mainly composed of PV generation system, ES. Among them, the PV generation system is consisted of N PV units, and a single PV unit is connected to the house-service bus through an inverter to provide power for the load [32]. The PV-BESS is formed by disposing the ES at the bus of the PV power station. which is shown in Fig. 2.

After the power grid blackout, the PV-BESS as the main control power supply of power grid system, the PV power station operates in the maximum power output mode. Energy Storage maintains voltage and frequency stability.

III. THE STRATIFIED OPTIMIZATION STRATEGY

At the beginning of black-start of PV-BESS, the randomness of PV output power leads to the uncertainty of the feasibility of black-start of PV-BESS. In the process of black-start of PV-BESS, the batch input of high power load and the fluctuation of PV make the over-charging and over-discharging of ES. Therefore, a stratified optimization strategy for black-start of PV-BESS is proposed in this paper, which can ensure that the PV output power meets the requirements of black-start power and provide enough power for the load at the same time.

A. FRAMEWORK OF STRATIFIED OPTIMIZATION STRATEGY

The Framework of stratified optimization strategy is shown in Fig. 3, which is divided into data analysis layer, optimization coordination layer and scheduling control layer. Among them, the data management mainly collects PV unit power, load power, ES status, and black-start operation instructions, as well as retrieves historical data of PV unit and numerical weather forecast information for the period to be predicted. The data analysis layer combines the data in the data management and evaluates the black-start of PV-BESS through the PV power prediction and PV power index to determine whether the black-start of PV-BESS is feasible. Optimizing coordination layer optimizes the system through MPC based black-start of PV-BESS control strategy, outputs reference values of PV cell number (N_r) and ES power (P_{ESS}). The scheduling control layer combines the reference

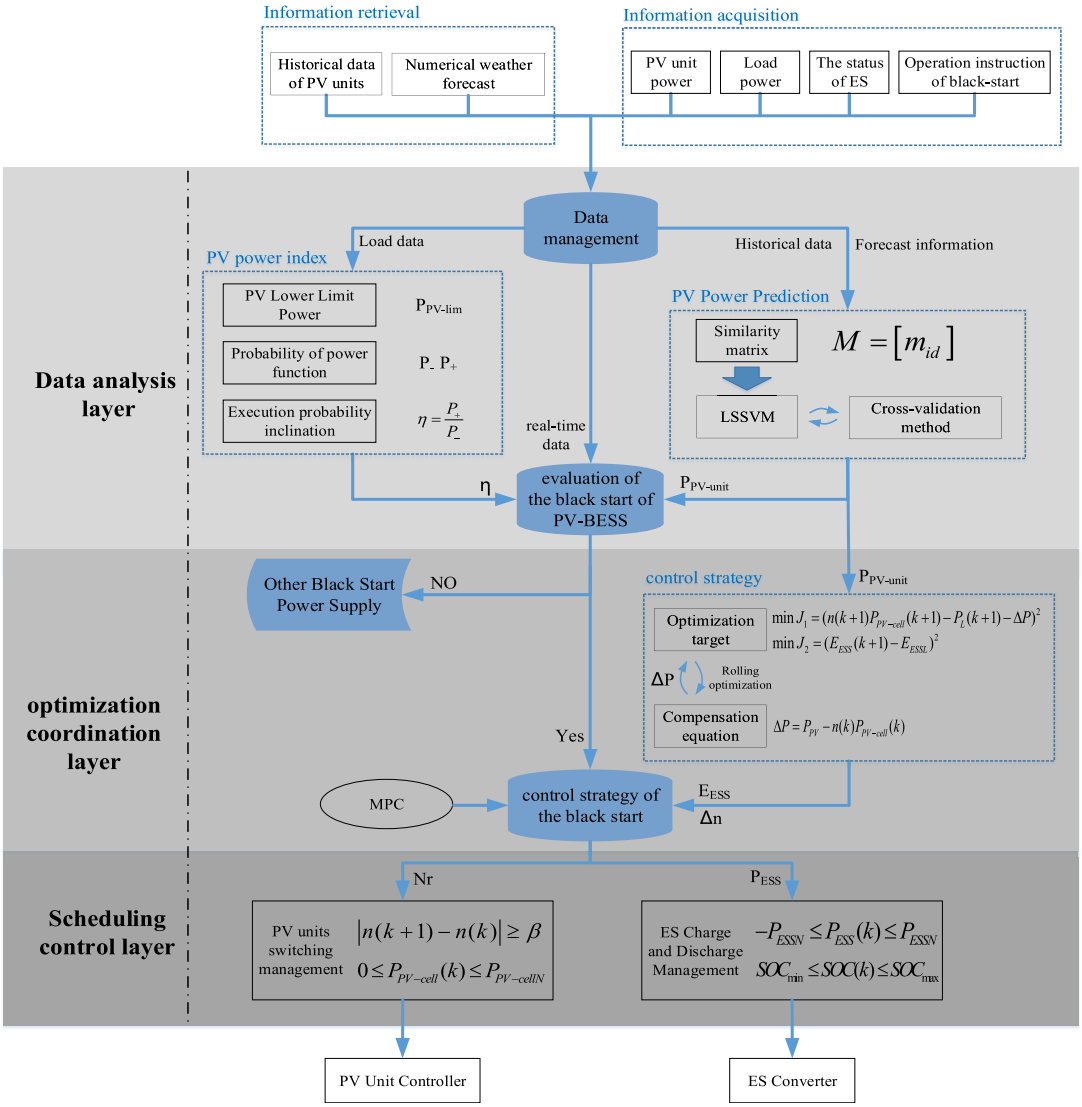

FIGURE 3. The framework of stratified optimization strategy for the PV-BESS. The framework of stratified optimization strategy is divided into data analysis layer, optimization coordination layer and scheduling control layer. Firstly, the feasibility of black-start of PV-BESS is calculated by data analysis layer. Then the optimal control quantity (N_r and P_{ESS}) is obtained by optimization coordination layer, and the scheduling control layer judges and controls the PV unit controller and the ES converter.

values of the number of PV cells and the reference values of charge/discharge power of ES to realize the switch-on management of PV cells and the charge/discharge power management of ES.

Among them: the data analysis layer is mainly based on the similarity matrix sorting method, designed a PV power prediction method suitable for black-start, and obtained the PV unit power reference value. Combining the lower limit power of PV power index, the probability inclination of black-start is calculated, and the feasibility of black-start is evaluated. The optimal coordination layer is mainly based on the correlation among PV, ES and load to establish a black-start mathematical model. Rolling optimization and real-time feedback are used to improve the accuracy of the model. The optimization objective is solved by MPC, and the optimal charge/discharge power of ES and the optimal number of PV cells at the k+1 time are obtained.

B. FUNCTIONAL DESIGN OF DATA ANALYSIS LAYER

Before the start of black-start, because of the randomness and uncertainty of PV power generation, whether the PV power station has sustained output capacity and whether the output power of PV power station meets the requirements of black-start load power are the key issues of black-start of PV-BESS. Therefore, this paper designs the data analysis layer. The data analysis layer is divided into two parts: PV power prediction and PV power index. Firstly, the reference value of PV output power is predicted by PV power prediction. Based on the reference value of PV output power, the PV power

index is calculated to evaluate the feasibility of black-start of PV-BESS.

1) IMPROVED PV POWER PREDICTION BASED ON BLACK-START PROCESS

The requirements of black-start process for PV power prediction are as follows: the black-start process lasts 30 to 60 minutes [16], so the ultra-short-term PV power prediction method is selected; in order to recover the load as soon as possible, the black-start process time should be reduced as much as possible, so the PV power prediction method needs shorter time and faster solution speed; and high accuracy of PV power prediction is required.

As a intelligent algorithm, Support Vector Machine (SVM) has been applied in PV power prediction in recent years, and the prediction accuracy based on SVM is relatively high [33]–[36]. Least Square Support Vector Machine (LSSVM) is an improved algorithm of Support Vector Machine (SVM), which can reduce the computational complexity and speed up the solution while ensuring the accuracy. Therefore, based on the similarity matrix sorting method, this paper improves the least squares support vector machine (LSSVM) prediction method so that the data analysis layer can predict the PV power of the next hour at the fastest speed with the premise of ensuring the accuracy.

The data analysis layer obtains the weather information of the future period through numerical weather forecast and filters the historical data by comparing the seasons and weather types and ranking the similarity matrix. The training samples with the highest similarity with the predicted days are obtained to improve the prediction accuracy. The prediction time scale is 1h, and the prediction flow chart is shown in Fig. 4.

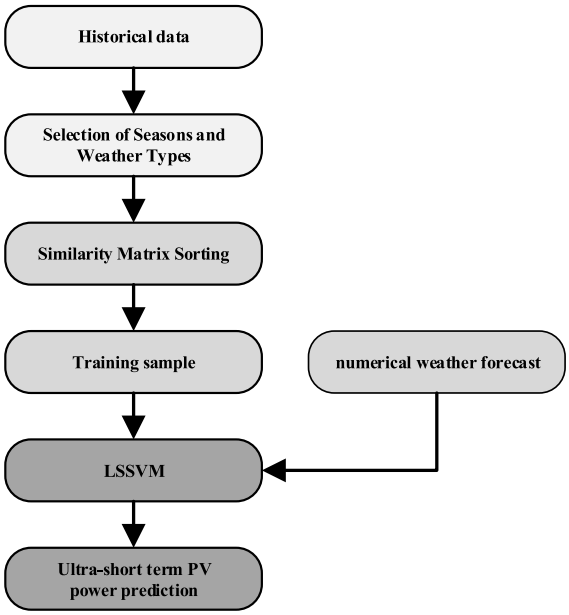

FIGURE 4. Flow chart of PV power prediction.

The selection of training samples and influencing factors (input variables) has a great impact on the prediction accuracy. The selection of training samples is to select the most similar data as training samples from the perspective of influencing factors (input variables).

2) SELECTION OF PREDICTIVE TRAINING SAMPLES

Considering four factors (including season, weather type, solar radiation intensity, and temperature), the similarity between each historical day and the day to be predicted is calculated, and the optimal training sample is selected.

Select the same season and weather type, the similarity matrix can be calculated in the same season and weather type data. According to the type of season, it can be divided into spring, summer, autumn, and winter. If the predicted day is the same as the historical day, $m = 0$, otherwise $m = 1$. According to the type of weather, it can be divided into sunshine, cloudy, and rain. If the predicted day is the same as the historical day, $m = 0$, otherwise $m = 1$.

Euclidean distance is used to describe the similarity of solar radiation intensity and temperature between historical and predicted days, as in (1).

$$m_d = \frac{\sqrt{\sum_{k=1}^{n} (x_{dk} - x_k)^2}}{n} \tag{1}$$

where: x_{dk} is the solar radiation intensity and temperature of d-day in historical day; x_k is the solar radiation intensity and temperature of the day to be predicted; n is the sampling point of the solar radiation intensity and temperature in a day.

The similarity matrix M is as shown in (2).

$$M = [m_{id}] \tag{2}$$

where: M is the similarity matrix; m_{id} is the similarity between each factor affecting the d-day and the predicted day.

Then the data in the table are normalized and the total similarity is as shown in (3).

$$F_d = \sum_{i=1}^{4} R m_{id} \tag{3}$$

where: F_d is the total similarity between the d-th historical day and the day to be predicted; R is the correlation coefficient.

Through sorting the total similarity of historical data, the training samples of SVM are selected.

The correlation coefficients of PV output power, solar radiation intensity and temperature are calculated by Pearson correlation coefficient formula, which are shown in Table 1.

The training samples selected by similarity matrix and the weather information obtained by numerical weather prediction are used as input of the least squares support vector machine (LS-SVM) prediction model to predict the output power of photovoltaic cells during the black-start process. After the reference output power at the factory bus of PV unit is predicted from PV power prediction, whether the PV power

TABLE 1. Correlation coefficient between PV power output and input variables.

Input variables	Correlation coefficient R
Solar radiation intensity S	0.8664
Temperature T	0.1652

meets the requirement of black-start power is calculated by the PV power index in the following section.

3) PV POWER INDEX

After predicting the reference value of PV output power, it is necessary to form a quantitative standard to evaluate whether the PV output power meets the requirement of black-start. For this reason, this paper designs an evaluation index of PV power based on probability inclination. Firstly, the lower PV limit power of black-start is determined. By calculating the probability inclination of PV power reference value, the feasibility of black-start of PV-BESS is obtained.

In the process of black-start, the output power of photovoltaic power station should satisfy the power of self-service system and provide power to the black-start load, as in (4).

$$NP_{\text{PV-}unit} \geq (1+\alpha)P_L \tag{4}$$

where: N is the number of PV units in PV power stations; $P_{PV-unit}$ is the predicted output power of PV unit; P_L is the auxiliary power of thermal power units; coefficient α a includes house-service electricity rate of PV, line loss per rate, and reserved margin, α is taken as 0.072.

This paper defines the lower limit of PV power in black-start, which is the minimum power P_{PV-lim} of PV units meeting the requirements of black-start power, as in (5).

$$p_{PV-\lim} = \frac{(1+\alpha)P_L}{N} \tag{5}$$

The execution process of the black-start is continuous in time. The power curves of PV cells predicted by PV power prediction are PV power function $f(P_{PV-unit})$, PV power function $f(P_{PV-unit})$ and PV lower limit power function $f(P_{PV-lim})$, as shown in (6) - (7).

$$\mathrm{P}_+ = \mathrm{P}(P_{PV-unit}) = \int_0^T f(P_{PV-unit})dv \tag{6}$$

$$\mathrm{P}_- = \mathrm{P}(P_{PV-\lim}) = \int_0^T f(P_{PV-\lim})dv \tag{7}$$

where: T is the black-start period; the relative size of the two indicates the degree of bias to execute feasibility, the inclination of execution probability is as shown in (8).

$$\eta = \frac{\mathrm{P}_+}{\mathrm{P}_-} \tag{8}$$

where: η is the executive probability inclination of black-start; When $\eta \geq 1$, the PV-BESS in black-start is relatively carried out. When $\eta < 1$, the PV-BESS in black-start is not relatively carried out. the over-charging and over-discharging of ES.

C. FUNCTION DESIGN OF OPTIMIZATION COORDINATION LAYER

In the black-start process, due to the input of high-power load and the fluctuation of PV output power, over-charging and over-discharging of ES occur, which leads to the failure of ES to continue to use. Model predictive control (MPC) can overcome the influence of time-varying and environmental uncertainties and is gradually applied to power system optimization control. At the same time, MPC can easily incorporate multiple constraints and can track multiple optimization objectives simultaneously. It is suitable for solving the problem of the coordinated control of PV and ES in black-start process.

The three elements of MPC are predictive model, rolling optimization and feedback correction. The principle of MPC is shown in Figure 5. Each axis represents time, the predictive time contains P time moments, and the control time contains M time moments, and P ≥M. At the current k-time, the optimal control command for the black-start of PV-BESS in the control time is obtained by solving the optimal problem in the control time on-line with the predicted data of the corresponding predictive time (P), and only the optimal control command for the first time (t=k+1) in the control time is executed.

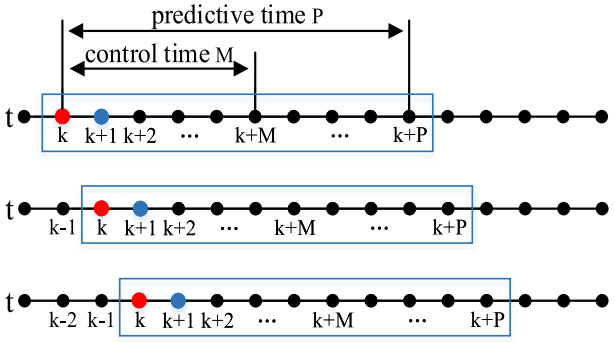

FIGURE 5. Rolling optimization time horizon of MPC. The predicted value of the predicted time (P) is solved at k time, and the optimal output control quantity (N_r and P_{ESS}) of the control time (M) is solved by the predicted value, and the control command (N_r and P_{ESS}) is applied at k+1 time.

In the black-start scene, the PV-BESS tracks the load directly. The PV-BESS needs to provide sufficient power for the load while maintaining the SOC of ES within a reasonable range until the black-start is completed. For this reason, this paper designs an optimal coordination layer based on Model Predictive Control (MPC). Firstly, the state-space model of black-start of PV-BESS process is established. Then, an optimal control method for load tracking by switching PV cells and ES assistant is proposed. In order to maximize the utilization of PV and the SOC of ES tracking the ideal value as the optimization goal, The number of PV cells and the power of energy storage is optimized by MPC, the reference values of the number of PV cells and the power of energy storage are obtained.

1) STATE SPACE MODEL

According to the theory of state space, assuming that the current time is k time, the state variables $x(k)$, the control variables is $u(k)$, the disturbance input is $r(k)$, the output variables is $y(k)$, the state space equation can be established, as in (9).

$$\begin{cases} x(k+1) = Ax(k) + B_1u(k) + B_2r(k) \\ y(k) = Cx(k) + D_1u(k) + D_2r(k) \end{cases} \tag{9}$$

Based on state space theory, a load tracking model of PV-BESS based on MPC is established. The power balance equation is as shown in (10).

$$P_L(k+1) = P_{PV}(k) + P_{ESS}(k) \tag{10}$$

where: $P_L(k+1)$ is the load power at k+1 time; $P_{PV}(k)$ is the total PV power at k time; $P_{ESS}(k)$ is the charge/discharge power of ES at k time.

Considering the real-time feedback in the process of energy optimization, the energy balance equation of ES is established, as in (11).

$$E_{ESS}(k+1) = E_{ESS}(k) - \Delta T_{ESS}P_{ESS}(k) \tag{11}$$

where: $E_{ESS}(k+1)$ is the ES capacity at k+1 time; $E_{ESS}(k)$ is the capacity actually collected at k time; ΔT_{ESS} is the conversion coefficient from kW to kWh.

Considering the method of switching PV units in conjunction with ES to track load, the number $N_r(k+1)$ of PV units at k+1 time can be obtained, as in (12).

$$N_r(k+1) = N_r(k) + \Delta N_r \tag{12}$$

where: $N_r(k)$ is the number of PV units actually collected at k time; ΔN_r is the change value of PV unit number.

Equations (10), (11), and (12) are transformed into state space models, as in (13).

$$\begin{cases} \begin{bmatrix} x_1(k+1) \\ x_2(k+1) \\ x_3(k+1) \end{bmatrix} = \begin{bmatrix} 0 & 0 & 0 \\ 0 & 1 & 0 \\ 0 & 0 & 1 \end{bmatrix} \begin{bmatrix} x_1(k) \\ x_2(k) \\ x_3(k) \end{bmatrix} \\ + \begin{bmatrix} 1 & 0 \\ -\Delta T & 0 \\ 0 & 1 \end{bmatrix} \begin{bmatrix} u_1(k) \\ u_2(k) \end{bmatrix} + \begin{bmatrix} 1 \\ 0 \\ 0 \end{bmatrix} [r(k)] \\ \begin{bmatrix} y_1(k) \\ y_2(k) \\ y_3(k) \end{bmatrix} = \begin{bmatrix} 1 & 0 & 0 \\ 0 & 1 & 0 \\ 0 & 0 & 1 \end{bmatrix} \begin{bmatrix} x_1(k) \\ x_2(k) \\ x_3(k) \end{bmatrix} \end{cases} \tag{13}$$

where: the state variables x_1, x_2, and x_3 are P_L, E_{ESS}, and N_r; the control variables u_1 and u_2 are P_{ESS} and ΔN_r; the disturbance input r is P_{PV}; the output variables y_1, y_2, and y_3 are P_L, E_{ESS}, and N_r.

2) OPTIMIZING OBJECTIVES

In each optimization cycle, The optimal values of the control variables (P_{ESS} and ΔN_r) are solved, which converted to static optimization in a fixed time. The optimization objectives are as follows:

In the black-start process, PV is the main black-start power supply. First, the difference between source and load is reduced by switching PV cells. Then, the fluctuation of PV output power is suppressed by ES. Therefore, the sub-objective function J_1 is designed: as in (14).

$$J_1 = \min \sum_{k}^{k+M} (N_r(k+1)P_{PV-unit}(k+1) - P_L(k+1) - \Delta P)^2 \tag{14}$$

where: $P_{PV-unit}(k+1)$ is the predicted PV unit power at k+1 time; ΔP is the compensation power.

Considering the power error caused by the PV power prediction error, the PV power at k+1 time is used to compensate the power error at k time. as in (15).

$$\Delta P = P_{PV} - N_r(k)P_{PV-unit}(k) \tag{15}$$

where: $P_{PV-unit}(k)$ is the power prediction value of PV units at k time.

ES is an auxiliary black-start power supply. From the point of view of ES itself, avoiding over-charging and over-discharging of ES is an important factor affecting the completion of black-start of PV-BESS. From the control point of view, controlling the ES capacity near the ideal value is conducive to the safe and smooth start of black-start of PV-BESS. Therefore, the sub-objective function J_2 is designed by:

$$J_2 = \min \sum_{k}^{k+M} (E_{ESS}(k+1) - E_{ESSL})^2 \tag{16}$$

where: E_{ESSL} is the ideal capacity of ES.

The objective function at all times should satisfy power balance constraints, ES output power constraints, PV unit output power constraints, and the SOC of ES constraints, which are shown in (17∼21), respectively. In order to prevent frequent switching PV units from introducing PV unit number change limit β, the reference value of PV unit number is given after optimizing the objective. By comparing the reference value with the current number of PV units, when the difference is greater than or equal to beta, the PV unit moves, and if it is less than beta, the PV unit does not move as shown in (21).

$$nP_{PV-unit}(k) + P_{ESS}(k) = P_L(k) \tag{17}$$

$$-P_{ESSN} \le P_{ESS}(k) \le P_{ESSN} \tag{18}$$

$$0 \le P_{PV-unit}(k) \le P_{PV-unitN} \tag{19}$$

$$SOC_{\min} \le SOC(k) \le SOC_{\max} \tag{20}$$

$$\Delta N_r \ge \beta \tag{21}$$

where: $P_L(k)$ is the load power at k time; P_{ESSN} is the rated power of ES; $P_{PV-unitN}$ is the rated power of PV units; SOC_{max} and SOC_{min} are the upper and lower limit of SOC of ES; $SOC(k)$ is the SOC of ES at k time; β is the change limit of the number of PV units.

The optimal charge/discharge power of ES and the optimal number of PV units at k+1 time are obtained by solving the optimization objective.

IV. SIMULATION VERIFICATION

Aiming at verifying the feasibility and validity of the stratified optimization strategy in different working conditions, the black-start process using the PV-BESS as the black-start power source is simulated by MATLAB/Simulink. The simulation time is 1 hour, Data sampling interval is 1 min. The numerical examples in this paper are derived from the measured data of a PV power station and a thermal power station in Hohhot. The load in the black-start process is auxiliary machines of the thermal power plant. In this paper, the simulation process is designed according to the starting sequence of auxiliary machine of thermal power plant. Take starting a 300MW thermal power unit as an example. The black-start simulation process is shown in Table 2.

TABLE 2. Black-start simulation process.

Time *t*/min	State of the System	Power of Input Load P_L/kW
t=0	Self-starting of PV-BESS	0
t=10	Input electrical pump	5500
t=20	Input circulation pump and condensate booster pump	2195
t=30	Input induced draft fan and forced draft fan	3240
t=40	Input primary air fan and Pulverized fuel exhauster	980
t=50	Input coal pulverizer	1000
t=60	The end of black-start process	0

In the simulation, the capacity of PV power station is 40 MWp, consisting of 40 1MWp PV units, and PV units number change limit β is 3. The rolling period M is 10min. The type of ES is lithium battery with 5.5 MW·h, the maximum charge/discharge power of ES is 15 MW, the initial SOC is 0.6, the SOC_{max} is 0.9, and the SOC_{min} is 0.1. The auxiliary units of thermal power plant are put into by batch operation, which is shown in Fig. 6. The total power of auxiliary units is 12.915 MW.

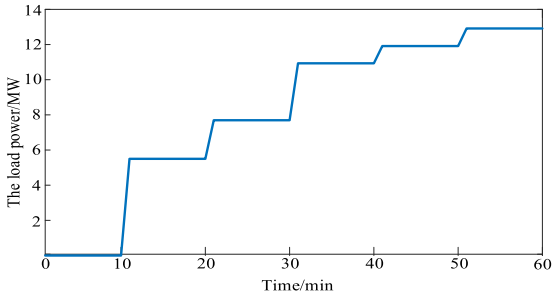

FIGURE 6. Load change curve in the black-start.

In this paper, the simulation process, first of all, the data analysis layer evaluates the PV output power during the black-start period to determine the feasibility of the black-start of PV-BESS. Then, the coordinated distribution of the output power of each power source and the status of the ES during the load input process are analyzed. In this paper, two power coordination modes are set up: mode one is to use the black-start control strategy in this paper, and to solve the optimal number of PV units and ES power through MPC; mode two is to use the traditional control method, select a certain number of PV units, start all at the beginning of the black-start process, and only use ES to assist the PV power station to track the load.

In order to verify the applicability of stratified optimization strategy for different PV output power, according to the influence of different weather types on PV output power, the weather types of Hohhot in 2016 are classified into sunny days, cloudy days, rain and snow days and overcast days [37]. Among them, the proportion of 157 days in sunny days is 42.9%, 118 days in cloudy days is 32.2%, 89 days in rain and snow days is 24.3% and 2 days in overcast days is 0.6%, as shown in Fig 7.

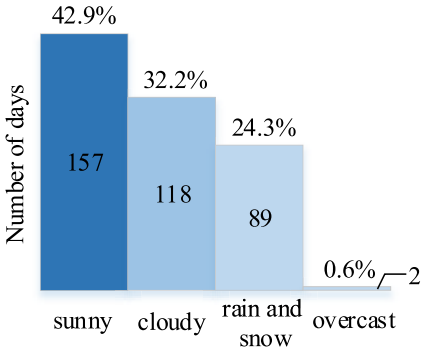

FIGURE 7. The proportion and days of weather types in Hohhot in 2016.

Among them, sunshine is abundant and PV output power is abundant in sunny days; PV output power decreases while fluctuation increases in cloudy weather affected by cloud shading; PV output power is the smallest and the largest fluctuation in rainy and snowy weather. Sunny, cloudy and snowy weather accounted for 99.4% of the year. Because of the small proportion of overcast days and the small fluctuation of PV output power, this paper chooses sunny, cloudy and snowy weather as typical weather types to simulate and verify.

Selecting 30 June 2016 (sunny), 5 May 2016 (cloudy) and 4 June 2016 (rainy) as typical days, assuming a blackout at 11:00, 11:00-12:00 is the black-start time. First, the output power of PV units in the black-start on typical day is predicted by LSSVM and back propagation neural network (BP). Meteorological information data are obtained from actual measurements of PV power stations. In this paper, the relative root mean square error rate (e_{RMSE}), the relative maximum error rate (e_{Rmax}) and accuracy rate are used as the basis for judging the prediction effect. Table 3 shows that the accuracy of the LSSVM method is higher than that of the BP method. The results obtained are in agreement with those in reference [33], [34].

TABLE 3. PV power prediction results.

Working condition	Relative root mean square error rate e_{RMSE}/%		Relative maximum error rate e_{Rmax}/%		Accuracy%	
	LSSVM	BP	LSSVM	BP	LSSVM	BP
Sunny day	4.90	7.21	8.19	14.32	90.41	82.33
Cloudy day	5.47	9.65	13.43	21.51	89.77.	78.11
Rainy day	7.14	12.14	16.05	28.41	84.39	75.39

A. BLACK-START SIMULATION ANALYSIS ON SUNNY DAY

With the PV output power predicted by the data analysis layer as a reference, the PV output power during the black-start period is evaluated to determine whether the PV output power meets the requirements of the black-start in sunny days. The predicted results are shown in Fig. 8. According to the method of Section 2, the lower limit power of PV is 346.1 kW, and the probability inclination of black-start of PV-BESS is 2.62 in typical sunny days from 11:00 to 12:00. Because the probability inclination of black-start of PV-BESS is greater than 1, it is known that the output power of PV meets the requirement of black-light storage start-up.

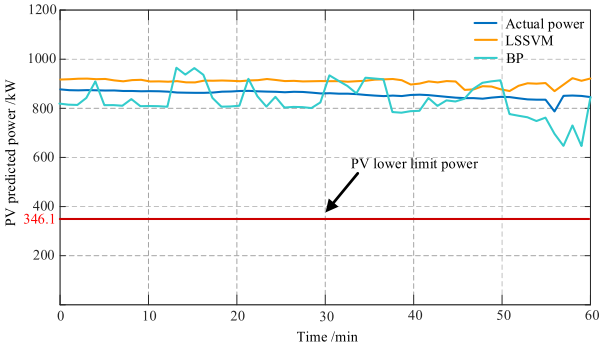

FIGURE 8. 1-hour power prediction curve of 1MWp PV cell on typical sunny day.

After confirming the feasibility of PV-BESS as black-start power supply, the simulation of black-start process of PV-BESS is carried out by combining two power coordination modes.

Under sunny conditions. In mode one, the optimization coordination layer controls the number of PV units and the charge/discharge power of ES, so that the PV-BESS tracks the load change. Fig. 9 shows that when t is 10 min, 20 min, and 30 min, the optimization coordination layer controls the PV unit controller, increases the corresponding number of PV units, and controls the output power of ES to suppress the fluctuation of PV output power fluctuation. When t is 40 min and 50 min, the number of PV units required to be increased is less than the limit of PV unit number change (β), in order to prevent frequently switching PV units, the number of PV

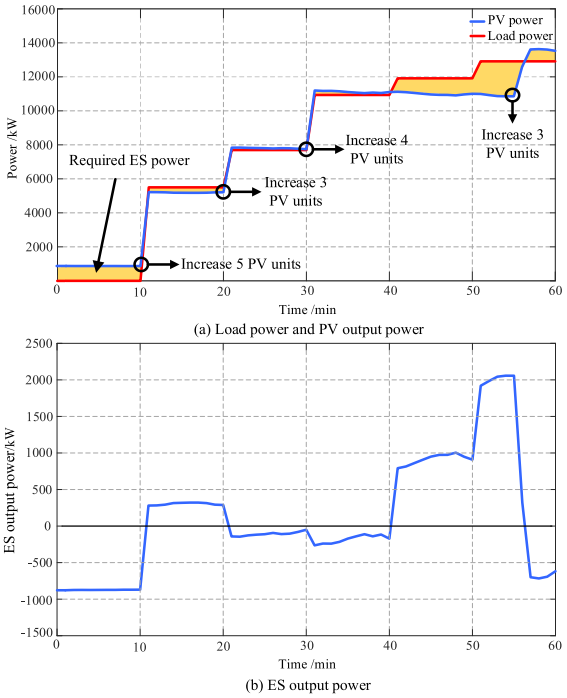

FIGURE 9. Output power of the PV-BESS running in mode one on typical sunny day.

units remains unchanged. When t = 55 min, the difference between load power and PV output power increases as PV output power decreases, so the optimization coordination layer controls the PV unit controller to increase three PV units, and the ES mode is changed from discharging mode to charging mode to maintain the SOC of ES at a reasonable level. The SOC of ES has been controlled between 0.5 and 0.7, following the ideal value of 0.6, as shown in Fig 11.

Under sunny conditions. In mode two, 16 PV units are determined according to formula (4) to meet the power requirement of black-start load, so 16 PV units are started at the beginning of black-start, and only ES is used to assist PV power station to track load. At t is 0-10 min, no load input, PV output power for ES charging, which is shown in Fig. 10. When t = 9 minutes, the SOC of ES reaches the upper limit of 0.9, as shown in Figure 11. Because there is no load input, the PV output power continues to charge the ES. After the ES reaches the upper limit of 0.9, the ES cannot absorb the excess PV output power, the power of the system is unbalanced, and the black-start of PV-BESS is forced to stop.

In the process of black-start of PV-BESS, according to the stratified optimization strategy in this paper, the feasibility of the black-start of PV-BESS is determined by data analysis layer, and then the number of PV units and the charge/discharge power of ES are controlled by the optimization coordination layer. By comparing and analyzing the two power coordination modes in black-start process, we can see that: the mode one is to coordinate ES and PV output power by optimizing the coordination layer so that the PV-BESS can track load well, and SOC of ES are kept in a reasonable state. In mode two, due to the sufficient PV output power

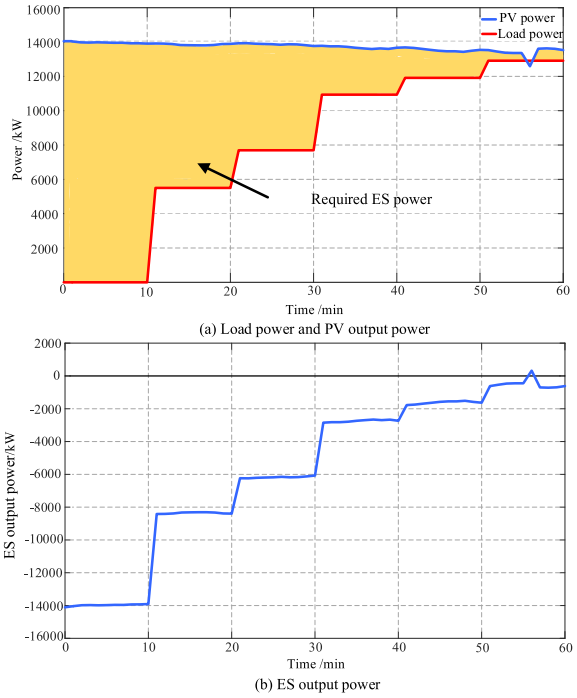

FIGURE 10. Output power of the PV-BESS running in mode two on typical sunny day.

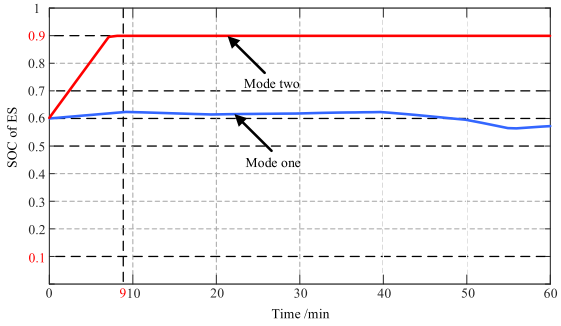

FIGURE 11. SOC curve of ES.

and small load input in the early stage, when the ES state reaches the upper limit of 0.9, the ES cannot absorb the excess PV output power, resulting in power imbalance, and the black-start process is forced to stop. The feasibility and effectiveness of the proposed strategy are verified.

B. BLACK-START SIMULATION ANALYSIS ON CLOUDY DAY

The probability inclination of typical days is calculated to determine whether the PV output power meets the requirements of black-start in cloudy weather. The predicted results are shown in Fig. 12. The method of Section 2 that the probability inclination of black-start of PV-BESS is 1.73 at 11:00-12:00 in the typical cloudy day. Since the probability inclination of black-start of PV-BESS is greater than 1, it is known that the output power of PV meets the requirement of black-start and can be used for black-start of PV-BESS.

After confirming the feasibility of PV-BESS used as black-start power supply, combining two power coordination

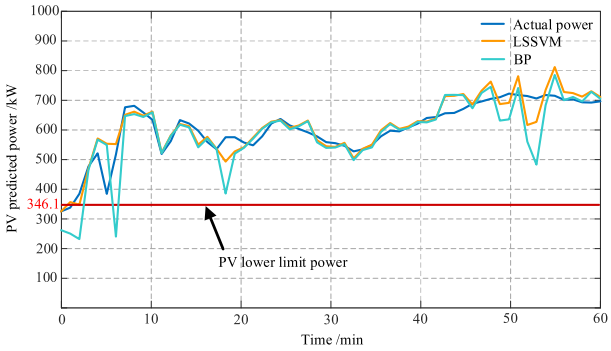

FIGURE 12. 1-hour power prediction curve of 1MWp PV cell on typical cloudy day.

modes, the simulation of black-start process is carried out on cloudy day.

Under Cloudy conditions. In mode one, the optimization coordination layer controls the number of PV units and the charge/discharge power of ES to make the PV-BESS follow the load change. As shown in Fig. 13, When t = 10 min, 20 min, and 30 min, due to the increase of load, the optimization coordination layer increases the corresponding number of PV units. At the same time, the output power of ES is controlled to suppress the fluctuation of PV output power fluctuation. When t = 40 minutes, the number of PV units needed is less than the limit of PV unit number change (β). In order to prevent frequent switching of PV units, the number of PV units remains unchanged. When t = 49min, due to the increase of PV output power and ES capacity, the optimization coordination layer cut off four PV units, and

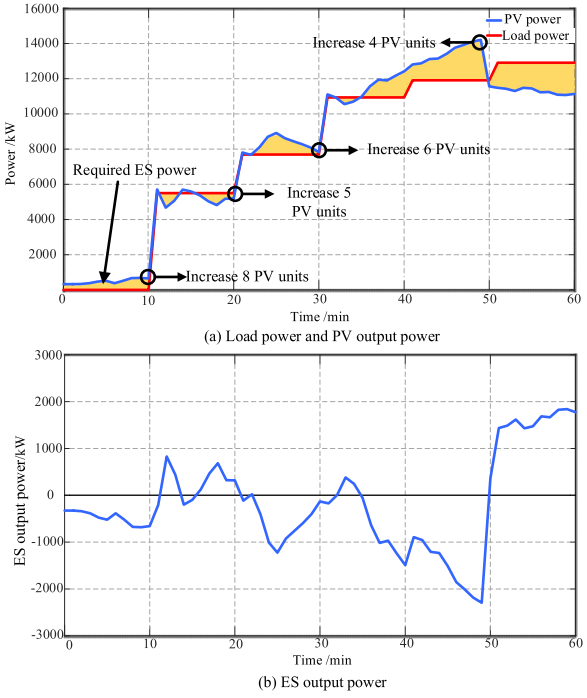

FIGURE 13. Output power of the PV-BESS running in mode one on typical cloudy day.

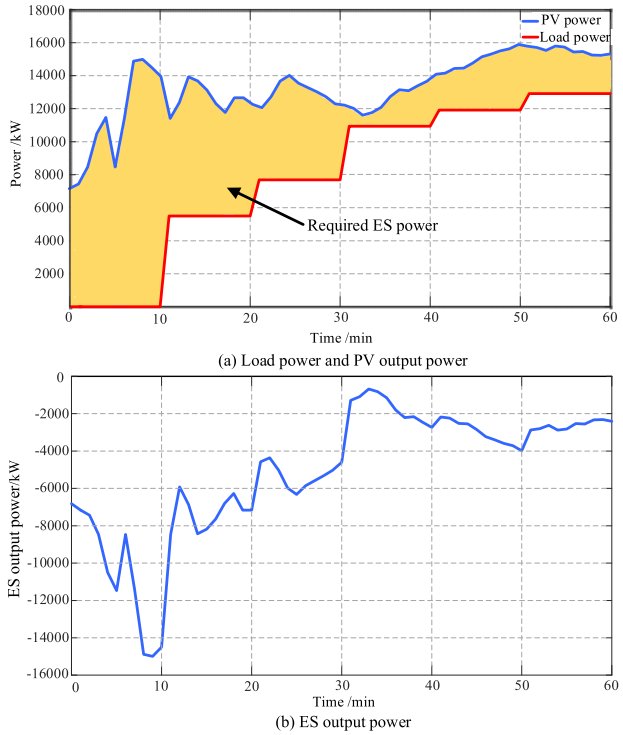

FIGURE 14. Output power of the PV-BESS running in mode two on typical cloudy day.

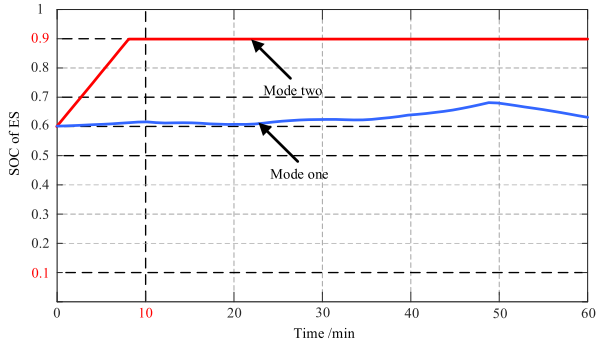

FIGURE 15. SOC curve of ES.

the ES mode is changed from charging mode to discharging mode. The SOC of ES has been controlled between 0.5 and 0.7, following the ideal value of 0.6, as shown in Fig 15.

Under Cloudy conditions. In mode two, 22 PV units are determined according to formula (4) to meet the power requirement of black-start load, so all 22 PV units are started at the beginning of black-start, and only ES is used to assist PV power station to track load. In t is 0-10 min, no load input, PV output power charge for ES, which is shown in Figure 14. When t = 10 minutes, the SOC of ES reaches the upper limit of 0.9, as shown in Figure 15. Because there is no load input, the PV output power continues to charge the ES. After the ES reaches the upper limit of 0.9, the ES cannot absorb the excess PV output power, the power of the system is unbalanced, and the black-start of PV-BESS is forced to stop.

The above simulation shows that in typical cloudy weather, the data analysis layer determines the feasibility of the black-start of PV-BESS firstly, and then through the comparison of mode one and mode two, it can be seen that the stratified optimization strategy can reasonably coordinate and control the output power of PV and ES to meet the load demand to achieve black-start, which verifies the feasibility and effectiveness of the proposed strategy.

C. BLACK-START SIMULATION ANALYSIS ON RAINY DAY

Taking the PV output power predicted by the data analysis layer as a reference, it is determined whether the PV output power meets the requirement of black-start on rainy days. The predicted results are shown in Fig. 16. The method of Section 2 that the probability inclination of the black-start of PV-BESS is 0.87 at 11:00-12:00 in typical rainy days. Because the probability inclination of the black-start of PV-BESS is less than 1, the output power of PV cannot meet the requirement of black-start, so the black-start of PV-BESS cannot be carried out.

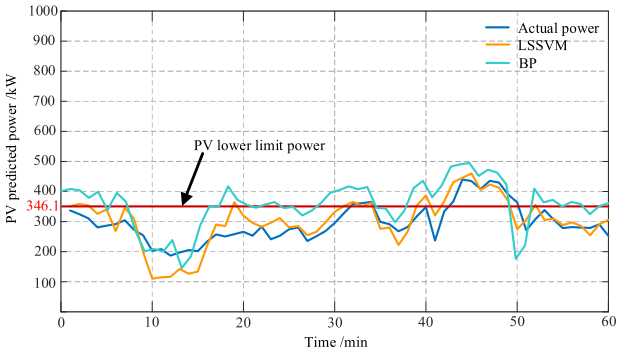

FIGURE 16. 1-hour power prediction curve of 1MWp PV cell on typical rainy day.

From the above simulation, we can see that in typical rainy days, the data analysis layer first evaluates the feasibility of the black-start of PV-BESS, because the PV output power is insufficient, so the PV-BESS cannot be used as the black-start power supply in this period.

From all the above simulations, it can be seen that in the typical sunny and cloudy days, the data analysis layer calculates that the probability inclination of black-start of PV-BESS is greater than 1, so the black-start of PV-BESS can be carried out; in the typical rainy days, the data analysis layer calculates that the probability inclination of the black-start of PV-BESS is less than 1, so the black-start of PV-BESS cannot be carried out. This is shown in Table 4.

TABLE 4. Feasibility assessment results for typical days.

Typical day	Sunny day	Cloudy day	Rainy day
Executive probability inclination	2.62	1.73	0.87
Is black-start executable	Yes	Yes	No

TABLE 5. Comparison of two power coordination modes.

Typical day	Sunny day		Cloudy day	
Power coordination mode	Mode one	Mode two	Mode one	Mode two
Average difference between PV power and load power/kW	136.94	5560.21	172.02	5125.91
Maximum difference between PV power and load power/kW	2057.95	14035.68	2291.99	14992.26
Mean deviation between SOC and ideal value	0.0083	0.28	0.028	0.27
Maximum SOC	0.62	0.9	0.68	0.9
Minimum SOC	0.56	0.6	0.6	0.6
Black-start result	Finish	Stop	Finish	Stop

In the black-start process on a typical sunny day, by comparing the two power coordination modes, it can be seen that the average and maximum difference between the PV and the load in mode one are 2.4% and 14.6% of that in mode two. The maximum and minimum SOC values of ES in mode one are 0.62 and 0.56, within the range of 0.5-0.7. In mode two, the maximum and minimum SOC values of ES are 0.9 and 0.6, and the ES is overcharged. Mode one completes the black-start, whereas mode two fails to complete the black-start due to overcharging of ES.

In the black-start process on a typical cloudy day, by comparing the two power coordination modes, it can be seen that the average and maximum difference between the PV and the load in mode one are 3.3% and 15.3% of that in mode two. The maximum and minimum SOC values of ES in mode one are 0.68 and 0.6, within the range of 0.5-0.7. In mode two, the maximum and minimum SOC values of ES are 0.9 and 0.6, and the ES is overcharged. Mode one completes the black-start, whereas mode two fails to complete the black-start due to overcharging of ES. From the comparison of different modes of the PV-BESS under different weather conditions, it can be seen that the optimization coordination layer reduces the depth of charge/discharge power of ES, prevents the over-charging and over-discharging of ES, and improves the utilization of PV. This is shown in Table 5.

The stratified optimization strategy proposed in this paper firstly evaluates the feasibility of the black-start of PV-BESS through data analysis layer, which can determine whether the output power of the PV-BESS can meet the power requirement of black-start load. Then the optimization coordination layer can effectively coordinate the output power of PV and ES, make the output power of the PV-BESS meet the load requirement, and prevent the over-charging and over-discharging of ES. The stratified optimization strategy in this paper can effectively evaluate the feasibility of the black-start of PV-BESS, and coordinate the output power of PV and ES to complete black-start.

V. CONCLUSION

When the PV-BESS is used as black-start power supply, due to the randomness of PV power generation, the uncertainty of the feasibility of black-start of PV-BESS, and the fluctuation of high-power load input and PV output power, the problem of over-charging and over-discharging of ES appears. In this paper, a stratified optimization strategy suitable for the black-start of PV-BESS is designed to make the output power of PV-BESS meet the requirements of black-start power, while the SOC of ES is kept in a reasonable range. A simulation verification of black-start of a local power grid with a high proportion of PV power supply is carried out based on MATLAB/Simulink.

The results of this study can be summarized as follows:

1) In this paper, a stratified optimization strategy suitable for the black-start of PV-BESS is designed, which mainly solves the uncertainties of the feasibility of the PV-BESS as black-start power supply and the problems of over-charging and over-discharging of ES. The data analysis layer based on PV power index and PV power prediction and the optimization coordination layer based on MPC are established respectively, which can ensure that PV output power meets the requirement of black-start power and provide enough power for load, and provide a reference for renewable energy to participate in black-start.
2) In view of the uncertainty of the feasibility of the PV-BESS as a black-start power source, the data analysis layer of stratified optimization strategy is designed in this paper. Firstly, based on similarity matrix sorting and combining the characteristics of black-start process, a PV power prediction method suitable for black-start is designed. Then, aiming at meeting the black-start load, a PV power index for the black-start of PV-BESS is proposed based on probability inclination, and the PV lower limit power of black-start is defined. The probability inclination of black-start is calculated by combining the PV lower limit power. The feasibility of black-start of PV-BESS is evaluated.
3) Aiming at the problem of over-charging and over-discharging of ES in the process of the black-start of PV-BESS, in this paper, an optimal coordination layer of stratified optimization strategy is designed. Firstly, the state-space model of the black-start of PV-BESS is established. Then, an optimal control method for load tracking by switching PV cells and ES assistant is proposed. The multi-objective optimization function is solved by MPC to control the output power of PV and ES so that the PV-BESS can provide sufficient power for the load under the condition of energy storage constraints.

In this paper, the feasibility of the black-start of PV-BESS and the coordinated operation of PV and ES are preliminarily studied, but the effects of load input and fluctuation of PV on voltage and frequency are not considered. Therefore, the control strategies of PV and ES need to be further studied in the

future. At the same time, after the black-start of PV-BESS, how the PV-BESS can be used for the subsequent restoration of the power grid needs to be further studied on the parallel technology between the PV-BESS and thermal power units in the future.

REFERENCES

[1] W. J. Liu, Z. Z. Lin, F. S. Wen, and G. Ledwich, "Intuitionistic fuzzy Choquet integral operator-based approach for black-start decision-making," *IET Generation, Transmiss. Distribution*, vol. 6, no. 5, pp. 378–386, May 2012.
[2] G. Patsakis, D. Rajan, I. Aravena, J. Rios, and S. Oren, "Optimal black start allocation for power system restoration," *IEEE Trans. Power Syst.*, vol. 33, no. 6, pp. 6766–6776, Nov. 2018.
[3] Y.-T. Chou, C.-W. Liu, Y.-J. Wang, C.-C. Wu, and C.-C. Lin, "Development of a black start decision supporting system for isolated power systems," *IEEE Trans. Power Syst.*, vol. 28, no. 3, pp. 2202–2210, Aug. 2013.
[4] A. Castillo, "Risk analysis and management in power outage and restoration: A literature survey," *Electr. Power Syst. Res.*, vol. 107, pp. 9–15, Feb. 2014.
[5] C. Xia, C. Li, H. Lan, Z. Du, and Y. Chen, "Frequency regulation strategy based on variable-parameter frequency limit control during black start," *IET Gener., Transmiss. Distrib.*, vol. 12, no. 17, pp. 4002–4008, Sep. 2018.
[6] M. C. Lian, Z. G. Dong, and S. Li, "The regional power grid black-start scheme evaluation based on TOPSIS," *J. Northeast Dianli Univ.*, vol. 34, no. 2, pp. 32–37, Apr. 2014.
[7] W. Sun, C.-C. Liu, and L. Zhang, "Optimal generator start-up strategy for bulk power system restoration," *IEEE Trans. Power Syst.*, vol. 26, no. 3, pp. 1357–1366, Aug. 2011.
[8] A. Ketabi, A. Karimizadeh, and M. Shahidehpour, "Optimal generation units start-up sequence during restoration of power system considering network reliability using bi-level optimization," *Int. J. Elect. Power Energy Syst.*, vol. 104, pp. 772–783, Jan. 2019.
[9] C. L. Moreira, F. O. Resende, and J. A. P. Lopes, "Using low voltage MicroGrids for service restoration," *IEEE Trans. Power Syst.*, vol. 22, no. 1, pp. 395–403, Feb. 2007.
[10] P. Mukhopadhyay, V. Pandey, A. P. Das, C. Kumar, P. A. R. Bende, K. K. Parbhakar, J. Agasty, R. P. Rakhia, and C. Felix, "Black start experiences for 400 kV hydro power plant in western regional grid of India," in *Proc. Nat. Power Syst. Conf. (NPSC)*, Bhubaneswar, India, Dec. 2016, pp. 1–6.
[11] Y. Liu, R. Fan, and V. Terzija, "Power system restoration: A literature review from 2006 to 2016," *J. Mod. Power Syst. Clean Energy*, vol. 4, no. 3, pp. 332–341, Jul. 2016.
[12] C. Li, S. Zhang, J. Zhang, J. Qi, J. Li, Q. Guo, and H. You, "Method for the energy storage configuration of wind power plants with energy storage systems used for black-start," *Energies*, vol. 11, no. 12, p. 3394, Dec. 2018.
[13] J. Li, X.-Y. Ma, C.-C. Liu, and K. P. Schneider, "Distribution system restoration with microgrids using spanning tree search," *IEEE Trans. Power Syst.*, vol. 29, no. 6, pp. 3021–3029, Nov. 2014.
[14] B. Zhao, X. Dong, and J. Bornemann, "Service restoration for a renewable-powered microgrid in unscheduled island mode," *IEEE Trans. Smart Grid*, vol. 6, no. 3, pp. 1128–1136, May 2015.
[15] J. Li, Y. Ma, G. Mu, X. Feng, G. Yan, G. Guo, and T. Zhang, "Optimal configuration of energy storage system coordinating wind turbine to participate power system primary frequency regulation," *Energies*, vol. 11, no. 6, p. 1396, May 2018.
[16] B. Zhang, P. Dehghanian, and M. Kezunovic, "Optimal allocation of PV generation and battery storage for enhanced resilience," *IEEE Trans. Smart Grid*, vol. 10, no. 1, pp. 535–545, Jan. 2019.
[17] G. B. M. A. Litjens, E. Worrell, and W. G. J. H. M. van Sark, "Economic benefits of combining self-consumption enhancement with frequency restoration reserves provision by photovoltaic-battery systems," *Appl. Energy*, vol. 223, pp. 172–187, Aug. 2018.
[18] W. Jing, C. H. Lai, W. S. H. Wong, and M. L. D. Wong, "A comprehensive study of battery-supercapacitor hybrid energy storage system for standalone PV power system in rural electrification," *Appl. Energy*, vol. 224, pp. 340–356, Aug. 2018.
[19] Z. Xu, P. Yang, Z. Zeng, J. Peng, and Z. Zhao, "Black start strategy for PV-ESS multi-microgrids with three-phase/single-phase architecture," *Energies*, vol. 9, no. 5, p. 372, May 2016.
[20] W. Liu, L. Sun, Z. Lin, F. Wen, and Y. Xue, "Multi-objective restoration optimisation of power systems with battery energy storage systems," *IET Gener. Transm. Distrib.*, vol. 10, no. 7, pp. 1749–1757, May 2016.
[21] X. U. Shaohua and L. I. Jianlin, "Grid-connected/island operation control strategy for photovoltaic/battery micro-grid," *Proc. CSEE*, vol. 33, no. 34, pp. 25–33, Dec. 2013.
[22] M. B. Delghavi, S. Shoja-Majidabad, and A. Yazdani, "Fractional-order sliding-mode control of islanded distributed energy resource systems," *IEEE Trans. Sustain. Enery*, vol. 7, no. 4, pp. 1482–1491, Oct. 2016.
[23] H. Shuai, J. Fang, X. Ai, J. Wen, and H. He, "Optimal real-time operation strategy for microgrid: An ADP-based stochastic nonlinear optimization approach," *IEEE Trans. Sustain. Enery*, vol. 10, no. 2, pp. 931–942, Apr. 2019.
[24] Q. Fu, A. Nasiri, V. Bhavaraju, A. Solanki, T. Abdallah, and D. C. Yu, "Transition management of microgrids with high penetration of renewable energy," *IEEE Trans. Smart Grid*, vol. 5, no. 2, pp. 539–549, Mar. 2014.
[25] P. Lin, Z. Peng, Y. Lai, S. Cheng, Z. Chen, and L. Wu, "Short-term power prediction for photovoltaic power plants using a hybrid improved Kmeans-GRA-Elman model based on multivariate meteorological factors and historical power datasets," *Energy Convers. Manage.*, vol. 177, pp. 704–717, Dec. 2018.
[26] W. Wei and Z. Shujian, "Analysis on the operation stability of photovoltaic inverter in weak grid," *J. Northeast Electr. Power Univ.*, vol. 38, no. 1, pp. 8–14, Feb. 2018.
[27] M. Ye, Y. Liu, X. Gu, S. Han, and Q. Hu, "Black-start value evaluation of wind power using a conditional risk method and its application," *Power Syst. Technol.*, vol. 42, no. 11, pp. 3796–3805, Nov. 2018.
[28] Y. Zhao, Z. Lin, Y. Ding, Y. Liu, L. Sun, and Y. Yan, "A model predictive control based generator start-up optimization strategy for restoration with microgrids as black-start resources," *IEEE Trans. Power Syst.*, vol. 33, no. 6, pp. 7189–7203, Nov. 2018.
[29] A. Sharma, D. Srinivasan, and A. Trivedi, "A decentralized multi-agent approach for service restoration in uncertain environment," *IEEE Trans. Smart Grid*, vol. 9, no. 4, pp. 3394–3405, Jul. 2018.
[30] M. Yang, X. Chen, J. Du, and Y. Cui, "Ultra-short-term multistep wind power prediction based on improved EMD and reconstruction method using run-length analysis," *IEEE Access*, vol. 6, pp. 31908–31917, Jun. 2018.
[31] L. Yingpei and H. Yaxin, "A coordinated control strategy of PV battery-energy storage hybrid power system for black-start," *Power Syst. Technol.*, vol. 41, no. 9, pp. 2979–2986, Sep. 2017.
[32] J. Li, T. Zhang, L. Qi, and G. Yan, "A method for the realization of an interruption generator based on voltage source converters," *Energies*, vol. 10, no. 10, p. 1642, Oct. 2017.
[33] H. A. Kazem and J. H. Yousif, "Comparison of prediction methods of photovoltaic power system production using a measured dataset," *Energy Convers. Manage.*, vol. 148, pp. 1070–1081, Sep. 2017.
[34] F. Wang, Z. Zhen, B. Wang, and Z. Mi, "Comparative study on KNN and SVM based weather classification models for day ahead short term solar PV power forecasting," *Appl. Sci.*, vol. 8, no. 1, p. 28, Jan. 2018.
[35] J. Li, J. K. Ward, J. Tong, L. Collins, and G. Platt, "Machine learning for solar irradiance forecasting of photovoltaic system," *Renew. Energy*, vol. 90, pp. 542–553, May 2016.
[36] C. Wang and J. Lei, "Ultra-short-term power output forecasting of distributed photovoltaic based on error classification," *South. Power Syst. Technol.*, vol. 9, no. 4, pp. 41–46, 2015.
[37] J. Tan, C. Deng, W. Yang, N. Liang, and F. Li, "Ultra-short-term photovoltaic power forecasting in microgrid based on Adaboost clustering," *Automat. Electr. Power Syst.*, vol. 41, no. 21, pp. 33–39, Nov. 2017.